Australian Journal of Basic and Applied Sciences, 4(10): 4857-4869, 2010
ISSN 1991-8178

Analysis of Thermomechanical Fatigue by using Finite Element Post-processing

[1]Achgaf Zineb, [2]Khamlichi Abdellatif, [3]El Bakkali Larbi and [4]Francisco Mata Cabrera

[1]Modelling and Simulation of Mechanical Systems Laboratory, Faculty of Sciences at Tetouan 93002, BP. 2121, M'hannech, Tetouan, Morocco.
[2]Modelling and Simulation of Mechanical Systems Laboratory, Faculty of Sciences at Tetouan 93002, BP. 2121, M'hannech, Tetouan, Morocco.
[3]Modelling and Simulation of Mechanical Systems Laboratory, Faculty of Sciences at Tetouan 93002, BP. 2121, M'hannech, Tetouan, Morocco,
[4]Polytechnic School of Almaden, 1 Square Manuel Meca, 13400 Almaden, Ciudad Real, Spain.

Abstract: Lifetime of a standard dog-bone specimen is assessed under the action of various thermomechanical fatigue loadings. Mechanical and thermal cycles were assumed to occur concurrently and the special effect of phasing between thermal cycles and strains cycles was emphasized. The methodology used is based on finite element post-processing analysis by specialized fatigue software package that takes into account damage from three primary sources: fatigue, oxidation and creep. A parametric study has shown that thermomechanical fatigue is not always more damaging than the isothermal case. In the range of parameters investigated the out-of-phase thermomechanical fatigue was found to be more severe than the in-phase one.

Key words: Fatigue, Thermomechanical loading, In-phase cycles, Out-of-phase cycles, Finite element method

INTRODUCTION

Mechanical properties of materials such as the tensile strength, the yield strength and Young's modulus depend on temperature. In general, these quantities decrease with increasing temperature, but this is not always the case because Young's modulus of some tempered steels increases slightly at mid temperatures before decreasing at high temperatures. The effect of high temperature on mechanical properties is linked to transformations of the material structure due to various processes. In general, such processes imply that inelastic deformation can occur more easily at elevated temperatures, so more plastic deformation and creep occur in the plastic zone of a fatigue crack. Fatigue properties are affected by temperature and oxidation process may also be activated. As a result, fatigue damage accumulation is expected to be enhanced when temperature increases.

The combined action of cyclic strains at high temperatures with time-dependent temperature variations applies in practice to specific structures such as turbine blades and motor components as they are exposed to high combustion temperatures and high vibratory and friction loads. In general, the temperature profile varies between a high operating temperature and a low temperature. Cyclic thermal stresses are then generated if the structure is constrained and could cause extra fatigue damage in the structure, yielding considerable complexity of the problem scenario as temperature and time become two additional variables.

Discarding situations where temperature transients are significant, temperature can be assumed to be uniform and the time variable can be neglected. This would occur if enough large cycling time is used. Working with a high cycling period, hot-section components of motors and aircraft engines could be assumed to be operating under concurrent static thermal cycles and static strain cycles.

Even within the framework of the above mentioned simplified assumptions, thermomechanical repeated loading is expected to cause, in contrast with isothermal cyclic loading, different material damage to the components and to lead eventually to their early failure.

Corresponding Author: Khamlichi Abdellatif, Modelling and Simulation of Mechanical Systems Laboratory, Faculty of Sciences at Tetouan 93002, BP. 2121, M'hannech, Tetouan, Morocco,
E-mail: khamlichi7@yahoo.es
Phone : +212 667795068, Fax : +212 539994500

Thermomechanical fatigue (TMF) is characterised by the fact that interaction between mechanical fatigue, creep and oxidation that are occurring under concurrent thermal cycles and strain cycles leads to complex damage mechanisms, (Zhuang *et al*., 1998). Thomas *et al*. (1982) had shown through experiments that TMF testing is more severe than isothermal testing conducted at the maximum temperature. Bill *et al*. (1984) had found that the lifetime of material specimens under in-phase thermomechanical cycling is well below isothermal creep-fatigue lives obtained for a number of temperatures belonging to the temperature range that had been investigated. Fatigue damage is dependent on the phase relationship between strain and temperature. This effect is also material dependent. In the special case of metal matrix composites undergoing low cycle fatigue, phase effect was discussed in (Halford *et al*., 1976).

Damage contributions related to TMF vary as function of temperature dependent material parameters and operating environmental conditions. These include maximum and minimum temperatures, temperature range, mechanical strain range, strain rate, the phasing of temperature and strain, dwell time, etc…

Laboratory testing techniques enable nowadays realistic simulations of loading cycles and allow for accurate representation of real service conditions of components subjected to fatigue phenomenon. There are two extreme thermomechanical situations that are generally considered; in-phase (IP) and out-of-phase (OP) cycles. Under IP cyclic loading, the maximum strain occurs at the same time as the peak temperature, and the minimum strain occurs at the minimum temperature. Under OP cycles, the maximum strain occurs at the minimum temperature, and minimum strain at the peak temperature. In general, both in-phase and out-of-phase stress and temperature cycles were found to be more damaging than isothermal stress cycles. Often, but not at all times, in-phase stress and temperature cycles were found to be more damaging than out-of-phase cycles.

Models for the prediction of TMF lifetime are needed in order to anticipate when to change the fatigue sensitive components. This will noticeably increase reliability and reduce serviceability costs. A large number of thermomechanical fatigue models were proposed in the literature for the prediction of TMF lifetime, (Zhuang *et al*., 1998). They are classified according to the three families: Damage Summation (DS), Strain-Range Partitioning (SRP), and Strain Energy Partitioning (SEP). Each model was derived for a particular use of a given material under specific ranges of temperature and cyclic strain. No versatile model could yet be used to predict in all circumstances lifetime under arbitrary thermomechanical loading. Moreover, when one considers surface roughness, lifetime could be found to vary by an amplitude factor of two between a smooth specimen and a rough one. Accuracy of predictions should then be considered under the inherent variability, present even in isothermal fatigue, which results from the specimen surface state or from inohomogeneities existing inside the specimen material. Uncertainties affecting fatigue lifetime should then be integrated at their proper value when making comparisons between experimental data and theoretical predictions.

In this work, fatigue damage resulting from complex thermomechanical loading acting on the structure of a standard dog-bone specimen is investigated. Finite element modelling of the part is performed, then the specialized fatigue post-processing software package, e-fatigue, was used to assess lifetime under various combinations of fatigue loadings where variable phasing between mechanical strain cycles and thermal cycles was used.

2. Modelling of TMF lifetime:

Different approaches have been introduced for the prediction of fatigue lifetime either in isothermal case or in TMF case, (Swanson *et al*., 1986) and (Gocmez *et al*, 2010). There are phenomenological models which relate measured total mechanical fields and lifetime without considering explicitly the different damaging mechanisms, (Gao *et al*., 2005). In this kind of approaches considerable experimental data is usually needed to identify the model parameters. To reduce the experimental effort to a strict minimum, rational approaches of modelling fatigue lifetime were considered. These include three families: damage partitioning based methods, crack growth based models and fatigue theories based on energetic approaches. In these all these approaches model parameters are identified from specific tests.

In cumulative damage based models, explicit consideration of the different damaging mechanisms is carried out, (Halford *et al*., 1976), (Neu and Sehitoglu, 1989), (Sehitoglu, 1990), (Lemaitre and Chaboche, 1990) and (Sehitoglu, 1992). In crack growth based models, life is related to local inelastic strains at the crack tip (Paris *et al*., 1961), (Newman, 1984) and (Christ *et al*., 2003). In energetic based fatigue theories, a relation between dissipated energy and the number of cycles to failure is assessed (Skelton, 1991) and (Skelton, 1993).

For the uniaxial isothermal case Gocmez *et al*. (2010) have reviewed the classical fatigue criteria. Since engineering components are rather likely to experience in reality multiaxial anisothermal loading, extensions of fatigue criteria such as those using the concept of critical plane were introduced to incorporate as a first step isothermal multiaxial loading. However extension to anisothermal loading, within the context of cumulative

damage based models, needs yet to be achieved by taking into account temperature dependency of material parameters. Gocmez *et al*. (2010) have extended energetic approaches to take into account mean stress effect in the context of TMF. However the application was focused on predicting life under uniaxial low cycle fatigue under OP-TMF. The extension to a multiaxial case has not yet been achieved.

From a practical point of view, damage strain partitioning based methods were recognized to be pertinent if one decides to estimate fatigue lifetime by performing finite element post-processing, (de Andres *et al*., 1999), (Gaiera and Dannbauera, 2003), (Kocabicak and Firat, 2004), (Lei, 2008) and (Sun and Shang, 2010). Strain damage partitioning method will be used in the following to perform prediction of TMF lifetime (Sehitoglu and Boismier, 1990) and (Sehitoglu, 1992) by means of finite element post-processing.

There are many active mechanisms in the TMF process. But, it is convenient to consider damage to result from three major sources: fatigue, oxidation and creep. Damage from each process is summed to obtain an estimate of the total fatigue life, N_f, according to the following equation

$$\frac{1}{N_f} = \frac{1}{N_f^m} + \frac{1}{N_f^{ox}} + \frac{1}{N_f^{cr}} \tag{1}$$

where N_f^m is the fatigue damage lifetime, N_f^{ox} the oxidation lifetime and N_f^{cr} the creep lifetime.

The fatigue damage process is driven by cyclic plastic strains where oxidation and creep effects could be neglected. Fatigue damage is dominant at high strain ranges, strain rates and low temperatures.

Oxidation damage can occur when an oxide layer forms on the surface material. This process which occurs more spontaneously at higher temperatures happens either in OP-TMF or in IP-TMF according to two major mechanisms. In the first case, the oxide layer forms when the surface is hot and in compression. The oxide layer becomes brittle at the lower temperature and during mechanical straining it cracks to expose new clean metal surfaces which will rapidly oxidize. In the second case, the oxide forms during the hot portion of the loading cycle while the material undergoes tension. Cooling after that will cause a buckling delamination that yields the oxide film to fracture and clean metal surfaces are then exposed. Oxidation during isothermal loading for low temperatures is hardly perceptible and is not an active failure mechanism as isothermal test had reflected it.

Creep damage result essentially from a diffusion process. Diffusion is highly temperature and time dependant. Maximum stress rather than strain range has a dominant role and the interaction of the strain rate and temperature has a strong influence on the stresses that are observed during cyclic loading.

The strain-life equation is the most common description mode of the fatigue damage process. This equation writes

$$\frac{\Delta\varepsilon}{2} = \frac{\sigma_f'}{E}\left(2N_f^m\right)^b + \varepsilon_f'\left(2N_f^m\right)^c \tag{2}$$

where σ_f' is the fatigue strength coefficient, b the Basquin's fatigue strength exponent, ε_f' the fatigue ductility coefficient, c the Coffin-Manson fatigue ductility exponent and E the Young's modulus.

The oxidation damage formulation due to Neu and Sehitoglu (1989a) and (1989b) predicts that oxide damage will occur when the strain range exceeds a threshold $\Delta\varepsilon_{mech} > \varepsilon_0$ for oxide cracking. Oxidation damage equation is given by

$$\frac{1}{N_f^{ox}} = \left(\frac{H_{cr}}{\Phi_{ox} K_{peff}}\right)^{-\frac{1}{\beta}} \frac{2\left(\Delta\varepsilon_{mech}\right)^{\frac{2}{\beta}+1}}{\dot{\varepsilon}^{1-\frac{\lambda}{\beta}}} \tag{3}$$

with

$$\Phi_{ox} = \frac{1}{t_c}\int_0^{t_c} \exp\left(-\frac{1}{2}\left(\frac{\dot{\varepsilon}_{th}/\dot{\varepsilon}_{mech}+1}{\xi_{ox}}\right)^2\right)dt \quad , \quad K_{peff} = \int_0^{t_c} D_0 e^{-\frac{\Delta H_{ox}}{RT}}dt$$

where ε_0 is the threshold strain for oxide cracking, t_c the cycle duration, H_{cr} a constant related to critical oxide thickness, β the mechanical strain range exponent and λ the thermal strain rate sensitivity exponent, ξ_{ox} the oxidation phasing constant for thermal and mechanical strains, ΔH_{ox} the activation energy for oxidation, K_{peff} the effective parabolic oxidation constant and D_0 a scaling constant for oxidation.

The phasing factor ξ_{ox} is introduced to account for the type of oxide cracking that can occur in either IP or OP loading. Phasing is represented by the ratio of thermal and mechanical strain rates $\dot{\varepsilon}_{th}/\dot{\varepsilon}_{mech}$. From laboratory tests the OP-TMF ($\dot{\varepsilon}_{th}/\dot{\varepsilon}_{mech} = -1$) showed the most oxidation damage, $\Phi_{ox} = 1$, while for the free expansion case $\dot{\varepsilon}_{th}/\dot{\varepsilon}_{mech} = \pm\infty$ no oxidation damage was observed, $\Phi_{ox} = 0$.

The creep formulation suggested by Neu and Sehitoglu (1989a) and (1989b) predicts damage according to the equation

$$\frac{1}{N_f^{cr}} = \int_0^{t_c} A_{cr}\Phi_{cr} e^{-\frac{\Delta H_{cr}}{RT}}\left(\frac{\alpha_1\bar{\sigma}+\alpha_2\sigma_m}{K}\right)^m dt \tag{4}$$

with

$$\Phi_{cr} = \frac{1}{t_c}\int_0^{t_c} \exp\left(-\frac{1}{2}\left(\frac{\dot{\varepsilon}_{th}/\dot{\varepsilon}_{mech}-1}{\xi_{cr}}\right)^2\right)dt$$

where ΔH_{cr} is the activation energy for creep, A_{cr} a scaling constant for creep, m the creep stress exponent, $\bar{\sigma}$ the equivalent stress, σ_m the hydrostatic stress, α_1 a stress state constant, α_2 a hydrostatic stress sensitivity constant, ξ_{cr} the creep phasing constant for thermal and mechanical strains and K is the drag stress.

The drag stress is an internal state variable that is related to the strength of the material. It is the stress that defines the transition from creep to plasticity dominated deformation. It is not constant but depends on the temperature, T. A linear temperature for the drag stress is often employed: $K = K_0 - K_1 T$ where K_0 is the back stress and K_1 the back stress temperature dependence. If no creep damage occurs in compression $\alpha_1 = 1/3$ and $\alpha_2 = 1$. From laboratory tests the IP-TMF ($\dot{\varepsilon}_{th}/\dot{\varepsilon}_{mech} = 1$) showed the most creep damage, $\Phi_{cr} = 1$.

3. Numerical Modelling of TMF:

The following methodology is used to derive a numerical modelling of TMF. At first, finite element modelling of a mechanical system component under specific applied mechanical loading cycles and temperature

cycles is performed. The most strained mesh point is identified. Total strains histories in that point are then extracted. The eFatigue system (https://efatigue.com/) is used after that for evaluating fatigue life of the considered structural component through using Fatigue Calculator. This fatigue software was designed and supported by the fatigue group at the University of Illinois and contains all of the technologies and tools needed for accurate fatigue assessments.

The mechanical system considered in this study is a standard dog-bone specimen which is used habitually to investigate experimentally TMF (Lawson *et al*., 1991) and (Velay, 2003). The specimen is axisymmetric with length $L = 126\times10^{-3}$ m and variable radius between $R_{min} = 7\times10^{-3}$ m and $R_{max} = 16\times10^{-3}$ m . Only the quarter of a meridian section of this specimen needs to be modelled. Finite element modelling is performed under assumption of 2-D axisymmetric deformation.

Elastic or elastic plastic strain cycles and thermal cycles are considered to act simultaneously on the specimen. The mechanical loading results from applying a tension pressure designated by P at the extremities of the specimen. To obtain a thermal stress loading under homogeneous uniform temperature distribution, the specimen was restrained against axial expansion by creating an interaction boundary condition at its axial edges.

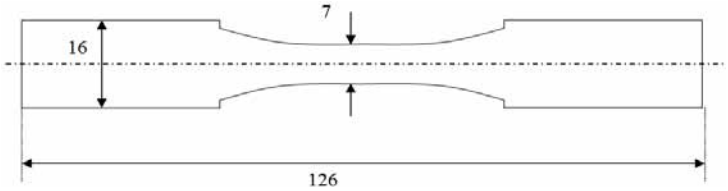

Fig. 1: Geometric configuration of the considered specimen

The material properties used are those of the SAE 1070 steel. This steel is considered in the temperature range 20°C and 600°C. The temperature dependent stress-strain curve for the SAE 1070 steel are defined according to Johnson and Cook's constitutive model (Johnson and Cook, 1989)

$$\sigma = (A + \kappa(\varepsilon_p)^n)\left(1 + B\log\left(\frac{\dot{\varepsilon}}{\dot{\varepsilon}_0}\right)\right)\left(1 - \left(\frac{T - T_r}{T_m - T_r}\right)^m\right) \quad (5)$$

where σ is the stress, ε_p the plastic strain, T the temperature, T_r is a reference temperature (the lowest temperature), T_m the melting temperature and $\dot{\varepsilon}_0$ a reference strain rate (the highest strain rate considered), A, κ, n, B and m are material constants.

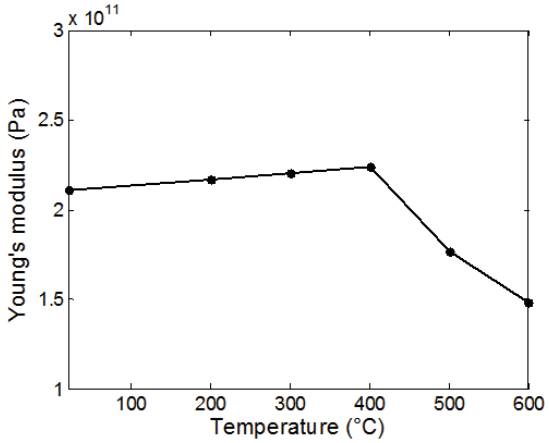

Fig. 2: Temperature dependant Young's modulus for the SAE 1070 steel in the range 20°C- 600°C

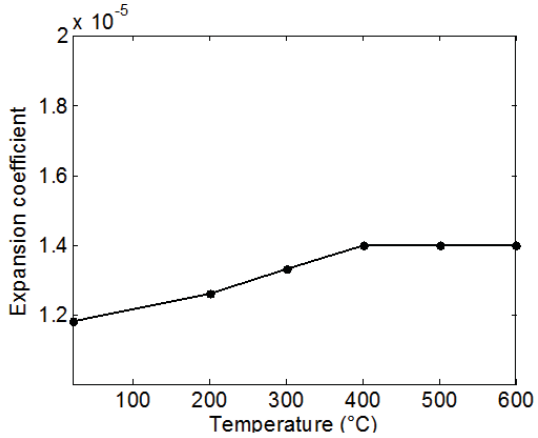

Fig. 3: Temperature dependant expansion coefficient for the SAE 1070 steel in the range 20°C- 600°C.

Temperature dependent data of this material in terms of respectively Young's modulus and the thermal expansion coefficient are given in figures 2 and 3, (Caccialupi, 2003). Poisson's coefficient does not depend on temperature and takes the constant value $\nu = 0.3$. Figure 4 presents the temperature dependent plastic curve of this material; significant dependency of the plastic behaviour on temperature can be observed.

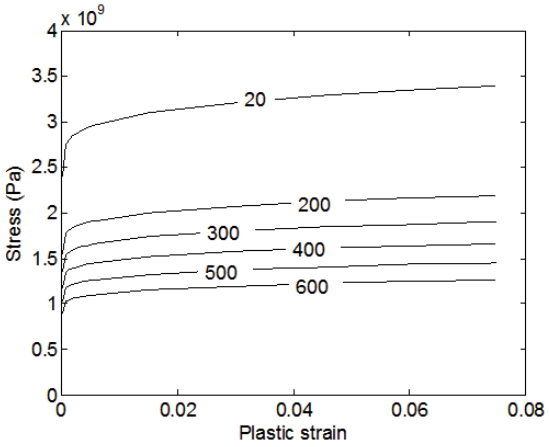

Fig. 4: The SAE 1070 steel curves giving stress versus plastic strain as function of temperature

The thermomecanical loading was applied according to either in-phase cycles, figure 5, or out-of-phase cycles, figure 6. Quantities considered to define the phasing are the applied tension and temperature. Both create positive axial strain at the vertical symmetry axis of the specimen.

Three different types of analyses were performed under Abaqus software:

- Isothermal mechanical loading containing tow cycles with constant amplitude strain cycles;
- In-phase thermomechanical loading containing two cycles with constant amplitude strain and constant amplitude thermal cycles;
- Out-of-phase thermomechanical loading containing two cycles with constant amplitude strain and constant amplitude thermal cycles.

Mesh refinement is one of the most important issues in the finite element simulation of fatigue stress concentration. Here, an adaptive remeshing technique integrating both energy and strain criteria was used. Beginning with a coarse mesh, figure 7, the initial mesh was refined to satisfy the asymptotic convergence condition. Figure 8 shows the refined mesh for a particular case of TMF loading.

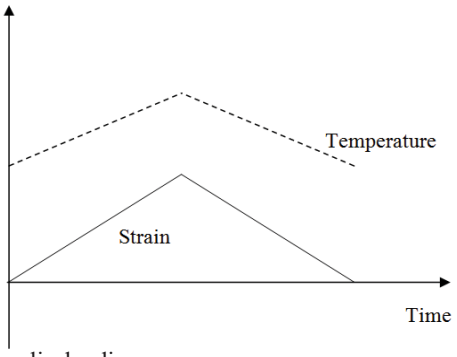

Fig. 5: Thermomechanical in-phase cyclic loading

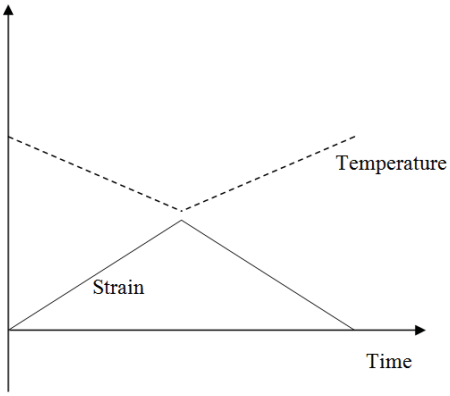

Fig. 6: Thermomechanical out-of-phase cyclic loading

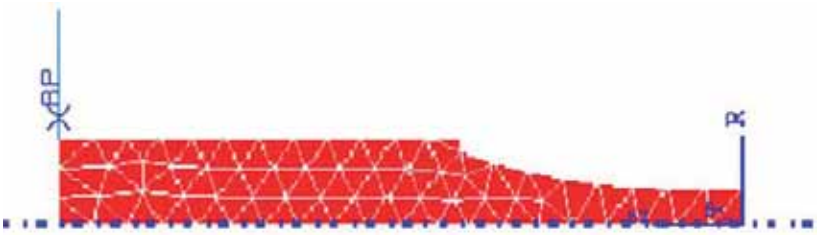

Fig. 7: Initial coarse mesh of the modelled portion of the specimen

Fig. 8: Refined mesh of the modelled portion of the specimen

Abaqus finite element results are analysed and the most strained point is determined. The total strain history at this point is extracted and transferred after that as input to fatigue post-processing software: Fatigue Calculator. In addition to strain cycles, user can define temperature cycles to be considered in TMF lifetime prediction. But, since the original TMF theory of Sehitoglu as formulated by equations (1-4) is one-dimensional and the dog-bone specimen is subjected to axisymmetric loadings, three-dimensional TMF model is needed. This is achieved by extending the one-dimensional theory to a three-dimensional state of stress using the concept of critical plane. The effective total strain is then used in equation (1) instead of the one-dimensional strain.

Fatigue Calculator provides the SAE 1070 fatigue material characteristics as a default option. These include fatigue, oxidation and creep characteristics. Using the units: MPa for E, σ'_f and K_0 and $^\circ C$ for temperature T, the following parameters were used during Fatigue simulations: $\alpha = 1.29\times10^{-5}$; $E(T) = 211000 + 34.2T$ si $T \le 400°C$; $E(T) = 224000 - 380T$ si $T > 400°C$; $K_0 = 256 + 0.0014T^2$ if $T < 304°C$; $K = 568 - 0.6T$ if $T \ge 304°C$; $n_1 = 5.4$; $n_2 = 8.3$; $A_0 = 4\times10^9$; $\Delta H_{in} = 210600$; E = 201 5 10 ; $\sigma'_f = 958$; $b = -0.093$; $\varepsilon'_f = 0.0996$; $c = -0.464$; $\xi_{cr} = 0.4$; $\Delta H_{cr} = 248100$; $A_{cr} = 1.562\times10^{14}$; $m = 11.34$; $\alpha_1 = 0.333$; $\alpha_2 = 1$; $\xi_{ox} = 2$; $\lambda = 0.75$; $\beta = 1.5$; $D_0 = 6.95\times10^7$; $\Delta H_{ox} = 156500$; $H_{cr} = 1.536\times10^{-2}$; $\varepsilon_0 = 0$.

RESULTS AND DISCUSSIONS

A parametric study was conducted on the specimen having the material data specified in the previous section under the following conditions:

- Three values of the pressure were applied: $P1 = 360MPa$; $P2 = 460MPa$ and $P3 = 560MPa$.
- For the isothermal case, the reference temperature was varied in the set $\{200; 300; 400; 500; 600\}$ (°C).
- For the IP-TMF or OP-TMF cases, the temperature range values were varied in the set $\{[200, 400]; [200, 500]; [200, 600]\}$ (°C).

The cycle duration was fixed at 240 s in order to limit time effects on creep and oxidation.

Pressures P1 and P2 were chosen to yield only elastic deformations in the whole dog-bone specimen when subject to isothermal loading, while pressure P3 is chosen to yield plastic deformations in the most loaded zone of the specimen: the central zone with small radius.

Using the finite element software Abaqus, the dog-bone specimen was modelled and the most loaded point identified. Strains either resulting from the applied pressure or from the temperature gradient were computed at that point. Fatigue computation for each case was then performed by means of eFatigue software.

Figure 9 gives the obtained equivalent strain for isothermal loadings as function of the applied pressure and temperature.

Figure 10 gives the obtained equivalent strain for IP-TMF loadings as function of the applied pressure and temperature range.

Figure 11 gives the obtained equivalent strain for OP-TMF loadings as function of the applied pressure and temperature range.

Figure 12 gives the obtained fatigue results in terms of the decimal logarithm of lifetime cycles for all the isothermal and TMF cases.

Figure 13 gives percentage damages associated to fatigue, oxidation and creep mechanisms for isothermal loadings as function of the applied pressure and temperature.

Figure 14 gives percentage damages associated to fatigue, oxidation and creep mechanisms for IP-TMF loadings as function of the applied pressure and temperature range.

Figure 15 gives percentage damages associated to fatigue, oxidation and creep mechanisms for OP-TMF loadings as function of the applied pressure and temperature range.

In the particular case of the dog-bone specimen and unlike what is largely known from literature dealing with TMF, figure 12 shows that the isothermal loading can be more damaging in some cases than the themomechanical loading. This is the case for example when the applied pressure is P1 for any considered temperature. But, this is not always the general rule since for pressure P3 and temperature 400°C the isothermal fatigue is less damaging than the IP-TMF.

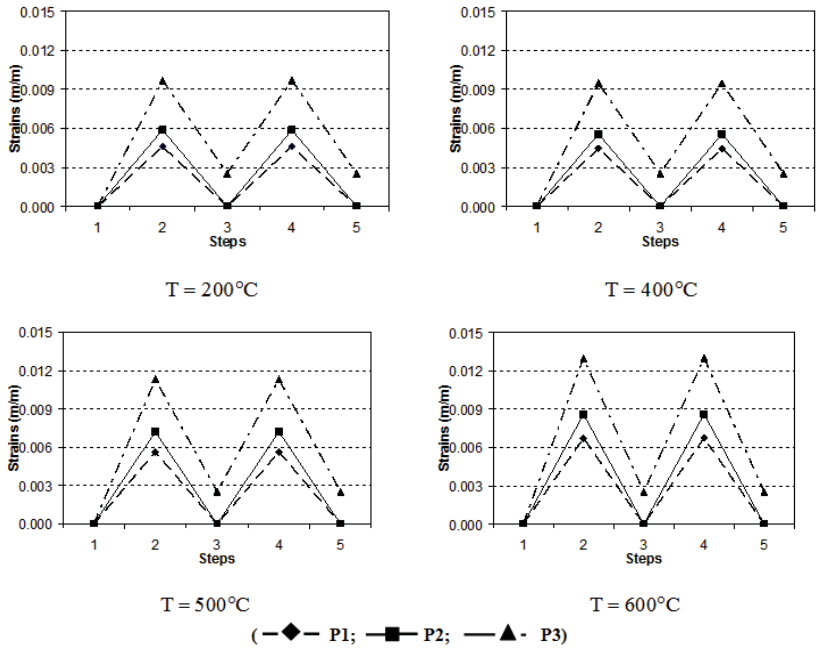

Fig. 9: Strains at the most loaded point of the specimen for the various isothermal loadings.

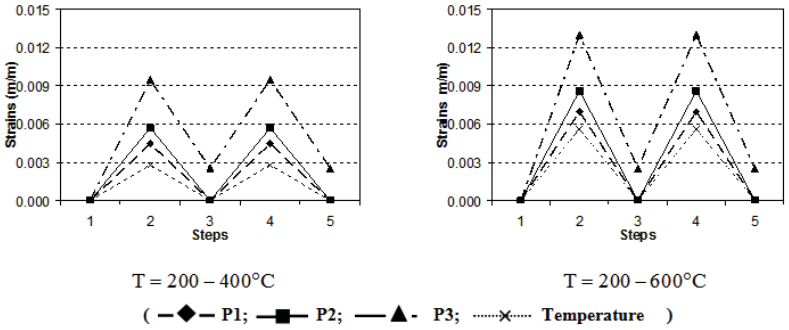

Fig. 10: Strains at the most loaded point of the specimen for the various TMF-IP loadings.

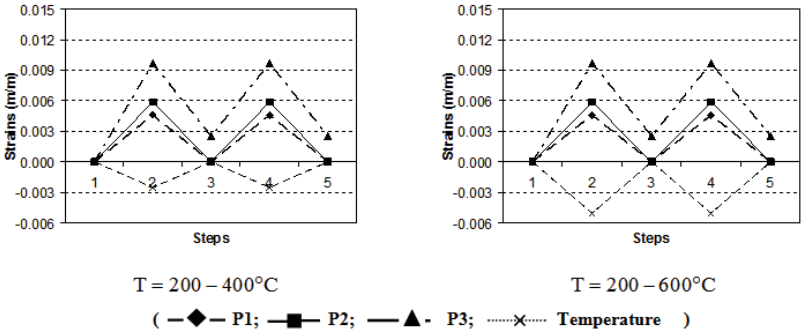

Fig. 11: Strains at the most loaded point of the specimen for the various TMF-OP loadings

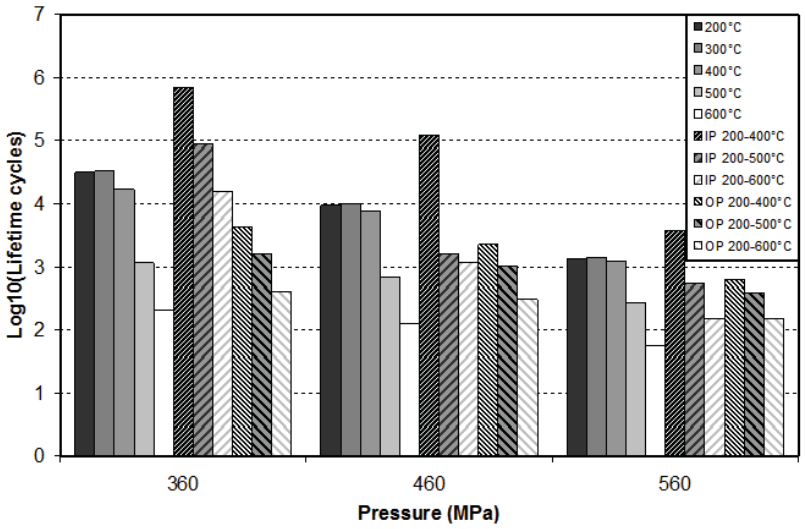

Fig. 12: The decimal logarithm of lifetime cycles for all cases as function of the applied pressure and temperature

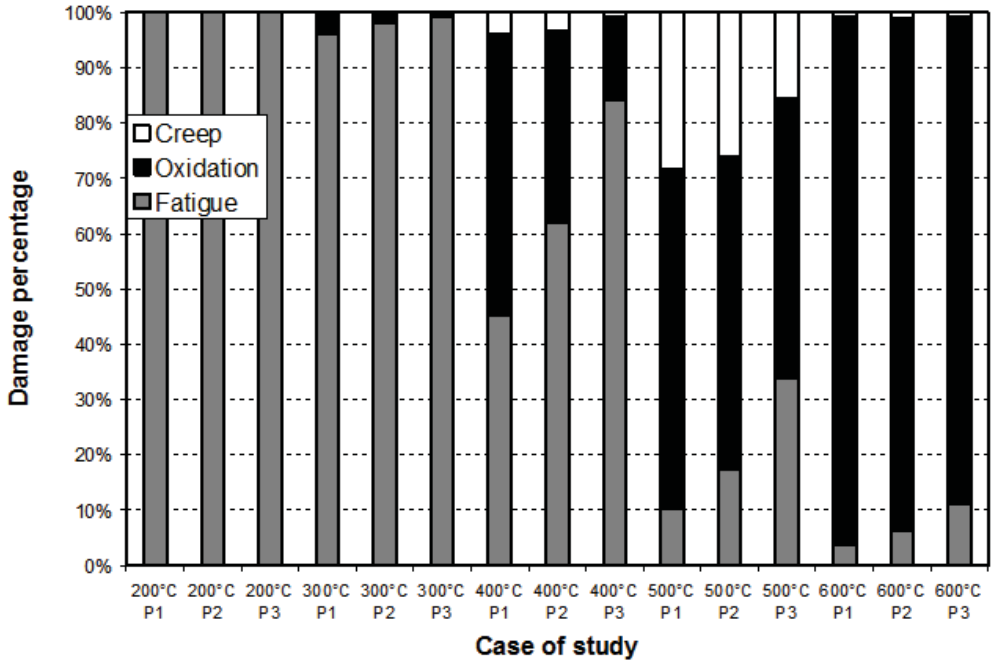

Fig. 13: Damage percentages associated to fatigue, oxidation and creep mechanisms for isothermal loadings as function of the applied pressure and temperature

The OP-TMF damage as shown in figure 12 was found, in most of the time, to be higher than that of the isothermal case with the same pressure and the same temperature range, but for pressure P3 the isothermal fatigue at 600°C is found to be more damaging than the OP-TMF fatigue in the temperature range 400°C and 600°C.

From figure 12, it can be noticed that almost all the time the OP-TMF damage is greater than that of the IP-TMF case. However for high pressures and high temperatures the difference between the In-Phase and Out-of-Phase cases decreases. As an example, for pressure P3 and temperature range 200-600°C there is no difference between the IP-TMF and the OP-TMF.

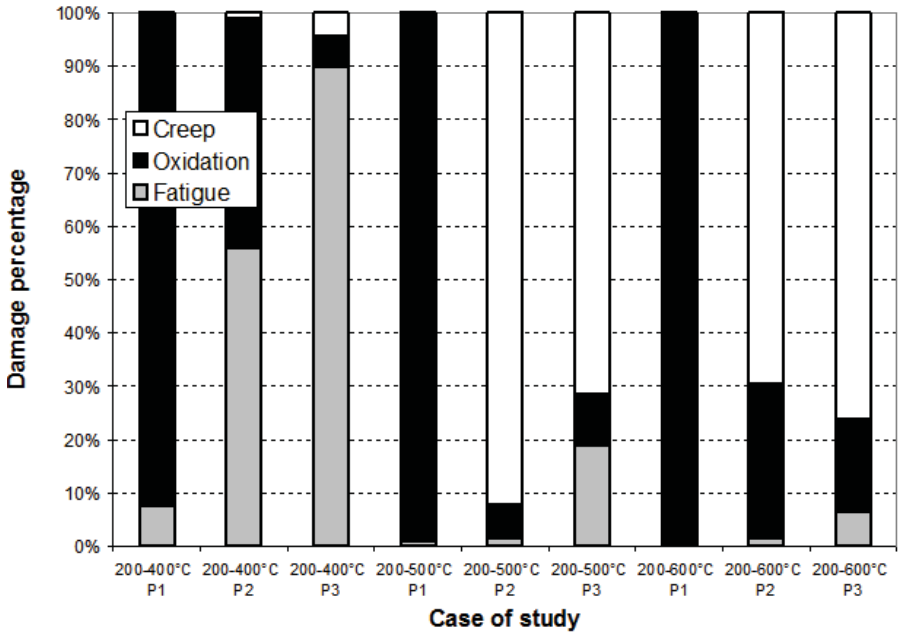

Fig. 14: Damage percentages associated to fatigue, oxidation and creep mechanisms for IP-TMF loadings as function of the applied pressure and temperature range

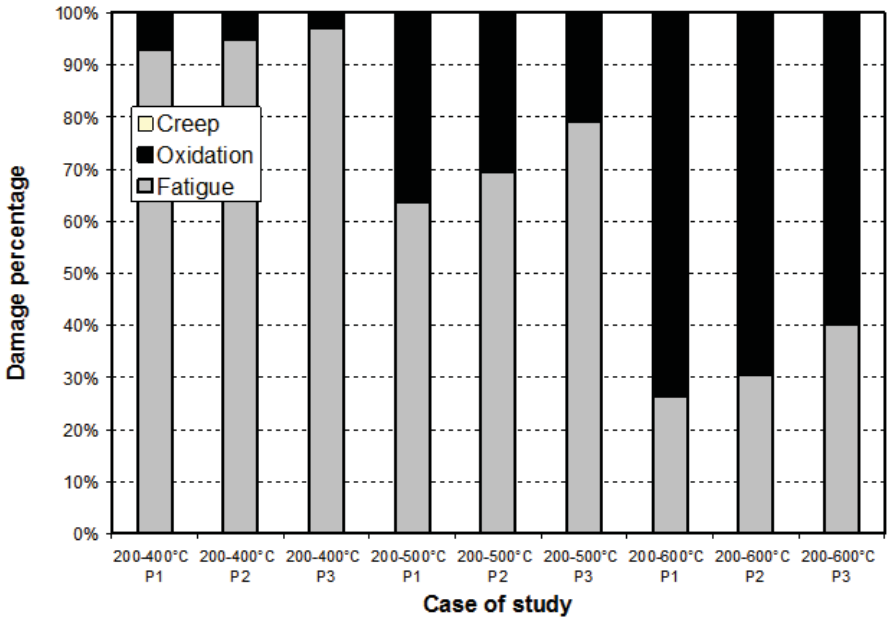

Fig. 15: Damage percentages associated to fatigue, oxidation and creep mechanisms for OP-TMF loadings as function of the applied pressure and temperature range

Considering now damage percentage associated to the various mechanisms of fatigue, it could be noticed from figure 13, in the isothermal case, that all the mechanisms: fatigue, oxidation and creep are present. Fatigue mechanism part dominates at lower temperatures and its effect increases with increasing pressure. Oxidation mechanism becomes important for temperatures exceeding 400°C and dominates damage for

temperatures higher than 500°C. Creep mechanism is present in the mid range interval of temperatures, between 400°C and 500°C, and disappears at 600°C.

Figure 14 shows that all the three mechanisms can be active in case of IP-TMF, with the fatigue mechanism being important for low temperatures and increasing with the applied pressure magnitude. The oxidation mechanism is important for low pressures while the creep mechanism dominates for high pressures.

Figure 15 shows that, in the case of OP-TMF, creep is a negligible damage mechanism while fatigue and oxidation are both very important. Fatigue dominates in all cases but oxidation is more active at high temperatures and low pressures.

Conclusions:

Lifetime of a standard dog-bone specimen with special boundary conditions and subjected to the action of various thermomechanical loadings was investigated by using finite element numerical modelling followed by fatigue post-processing. Numerical simulations have shown that thermomechanical fatigue is not always more damaging than isothermal fatigue. The in-phase cycles were found to reduce considerably damage in the specimen for low pressures and low temperatures in comparison with the isothermal case while out-of-phase cycles had yielded more damage than the isothermal case in all the investigated conditions, except one occurring at high temperature and high pressure. For high temperature and pressure only small differences appear between in-phase and out-of-phase scenarios.

All the damaging mechanisms was recognized to be active for the isothermal fatigue with fatigue to dominate at high pressures and low temperatures, while oxidation and creep effects were found to increase rapidly with increasing temperature. Oxidation dominated the out-of-phase fatigue cycling and creep the in-phase fatigue cycling.

ACKNOWLEDGMENTS

The authors would like to thank the Moroccan CNRST for having supported part of this research under student grant D2/001.

REFERENCES

Bill, R., M. Verrilli and G.R. Halford, 1984. A Preliminary study of the Thermo-Mechanical Fatigue of Polycrystalline MAR M-200, NASA TP-2280, AVSCOM TR 83-C-6.

Caccialupi, A., 2003. Systems development for high temperature, high strain rate material testing of hard steels for plasticity behavior modelling. MS in Mechanical Engineering, Georgia Institute of Technology.

Christ, H.J., A. Jung, H.J. Maier and R. Teteruk, 2003. Thermomechanical fatigue - Damage mechanisms and mechanism-based life prediction methods. Sadhana, 28(1-2): 147-165.

De Andres, A., J. Perez, M. Ortiz, 1999. Elastoplastic finite element analysis of three-dimensional fatigue crack growth in aluminium shafts subjected to axial loading. Int J Solids Struct., 36: 2231-2258.

Gaiera, C. and H. Dannbauera, 2003. Fatigue analysis of multiaxially loaded components with the FE-postprocessor FEMFAT-MAX. European Structural Integrity Society, 31: 223-240, doi:10.1016/S1566-1369(03)80013-4.

Gao, Z., W. Sun, Y. Wang and F. Zhang, 2005. Fatigue crack growth properties of typical pressure vessel steels at high temperature. 18th International Conference on Structural Mechanics in Reactor Technology (SMiRT 18), Beijing, China, August 7-12.

Gocmez T., A. Awarke and S. Pishinger, 2010. A new low cycle fatigue criterion for the isothermal and out-of-phase thermomechanical loading, International Journal of Fatigue, 32: 769-779.

Halford, G.R., S. Manson, B. Prillhofer, G. Winter and W. Eichlseder, 1976. Life prediction of thermal–mechanical fatigue using strain range partitioning, thermal fatigue of materials and components. ASTM STP, 612: 239-254.

Johnson, G.R. and W.H. Cook, 1985. Fracture characteristics of three metals subjected to various strains, strain rates, temperatures and pressures. Engineering Fracture Mechanics, 21(1): 31-48.

Kocabicak, U., M. Firat, 2004. A simple approach for multiaxial fatigue damage prediction based on FEM post-processing. Materials and Design, 25: 73-82. doi:10.1016/S0261-3069(03)00157-2.

Lawson, L., M.E. Fine and D. Jeannotte, 1991. Thermomechanical fatigue of a lead alloy Metallurgical and Materials Transactions A., 22(5): 1059-1070. doi: 10.1007/BF02661099.

Newman, Jr., 1984. A crack opening stress equation for fatigue crack growth. International Journal of Fracture, 24: 131-135.

Lei, Y., 2008. Finite element crack closure analysis of a compact tension specimen. International Journal of Fatigue, 30: 21-31.

Lemaitre, J. and J.L. Chaboche, 1990. Mechanics of solid materials, Cambridge: University Press, Cambridge.

Neu, R. and H. Sehitoglu, 1989. Thermo-Mechanical Fatigue, Oxidation and Creep: Part 1-Experiments. Met. Trans. A, 20A: 1755-1767.

Neu, R. and H. Sehitoglu, 1989. Thermo-Mechanical Fatigue, Oxidation and Creep: Part 2-Life Prediction. Met. Trans. A, 20A: 1769-1783.

Paris, P.C., M.P. Gomez and W.E. Anderson, 1961. A rational analytical theory of fatigue. The Trend of Engineering, 13: 9-14.

Sehitoglu, H., 1992. Thermo-Mechanical Fatigue Life Prediction Methods. Advances in Fatigue Lifetime Predictive Techniques, ASTM STP., 1122: 47-76.

Sehitoglu, H. and D.A. Boismier, 1990. Thermo-Mechanical Fatigue of Mar-M247: Part 2-Life Prediction. J. Eng. Mat. and Tech., 112: 80-89.

Skelton, R.P., 1991. Energy criteria for high temperature low cycle fatigue. Mater Sci Technol., 7: 427-439.

Skelton, R.P., 1993. Cyclic hardening, softening and crack growth during high temperature fatigue. Mater Sci Technol., 9: 1001-1008.

Sun, G.Q., D.G. Shang, 2010. Prediction of fatigue lifetime under multiaxial cyclic loading using finite element analysis. Materials and Design, 31: 126-133. doi:10.1016/j.matdes.2009.06.046.

Swanson, G.A., I. Linask, D.M. Nissley, P.P. Norris, T.G. Meyer, K.P. Walker, 1986. Life prediction and constitutive models for engine hot section, Anisotropic materials program. NASA contractor report 174952.

Thomas, G., J. Bressers and D. Raynor, 1982. Low-Cycle Fatigue and Life Prediction Methods. High Temperature Alloys for Gas Turbines, R. Brunetaud, Ed., D. Riedel Publishing Co., Netherlands, pp: 291-317.

Velay, V., 2003. Modélisation du comportement cyclique et de la durée de vie d'aciers à outils martensitiques. Ph.D. thesis, Ecole des Mines de Paris, 2003, Paris, France.

Zhuang, W.Z., N.S. Swansson, 1998. Thermo-mechanical fatigue life prediction: a critical review. Airframes and engines division/aeronautical and maritime research laboratory, DSTO-TR-0609.